18th International Conference on Information Fusion
Washington, DC - July 6-9, 2015

Automated State and Dynamics Estimation in Dynamically Mismodeled Systems with Information from Optimal Control Policies

Daniel P. Lubey
Department of Aerospace Engineering Sciences
University of Colorado
Boulder, Colorado 80309-0431
Email: daniel.lubey@colorado.edu

Daniel J. Scheeres
Department of Aerospace Engineering Sciences
University of Colorado
Boulder, Colorado 80309-0431
Email: scheeres@colorado.edu

***Abstract*—While observation sets for an individual object in orbit can be quite data-sparse, the sheer number of objects in orbit makes the tracking problem as a whole data-rich. As such it is infeasible for humans to process these measurements manually. While orbit determination procedures are largely automated the resulting solutions can be quite poor when the assumed dynamics are flawed due to mismodeled perturbations or unmodeled active maneuvers. This paper presents an automated version of the Optimal Control Based Estimator (OCBE) as applied to problems in the field of Space Situational Awareness. The OCBE algorithm supplements a state and dynamic estimation process with information from optimal control policies to create an estimator that is robust to dynamic mismodeling. This estimator is made adaptive through a maneuver detection based approach resulting in an algorithm that automatically estimates the system's state, detects dynamic mismodeling, and reconstructs that mismodeling. Along with a derivation and discussion of this algorithm, numerical simulations are provided to demonstrate this algorithm's ability to accurately track a spacecraft with mismodeled dynamics while simultaneously detecting and reconstructing those mismodelings.**

I. INTRODUCTION

Tracking objects around Earth is fraught with complications. With nearly 17,000 objects currently being tracked by U.S. Space Surveillance Network [1] it becomes a significant challenge to track a single object amongst the rest, as well as predict potential collisions amongst all of the objects. Additionally, over 75% of these objects are either spent rocket bodies or pieces of debris, which do not have well known physical properties (e.g. size, shape, reflectivity, etc.). Combined with the fact that the measurements are noncooperative (i.e. no direct communication with the object) this creates problems with object identification, association of uncorrelated tracks, and dynamic mismodeling since object dependent perturbations would be unknown (e.g. atmospheric drag, solar radiation pressure, etc.). While Space Situational Awareness (SSA) is a data-rich problem as a whole, the tracking of a single object is rather data-sparse - generating correlated measurements often every few orbits or less. This only compounds these problems further.

With all of these challenges, there is a clear need for state estimation algorithms that: (1) are robust to dynamic mismodeling, (2) are capable of detecting the presence of dynamic mismodeling, (3) provide reconstructions of mismodeled dynamics to correct the model for future times, and (4) are automated to perform all estimations without user input beyond initial conditions. In previous papers [2], [3], the authors developed the Optimal Control Based Estimator (OCBE) algorithm - a state estimator imbued with dynamic uncertainty properties that yield simultaneous control estimates that can be used to detect and reconstruct mismodelings in the dynamics. This algorithm has the first three desirable properties, but in its initial form it was not automated. In this paper we develop a method to automate the OCBE, such that the assumed dynamic uncertainty (a tunable parameter in the OCBE) is automatically selected with each new observation. This method will be based upon the the dynamic mismodeling identification properties of the estimator, otherwise known as maneuver detection.

The topics of Maneuver Detection and Reconstruction have been well-studied, but the resulting algorithms have generally been aimed at highly dynamical systems (such as missile tracking and guidance) and environments that are data-rich. Methods such as Bar-Shalom and Birmiwal's Variable Dimension Filter [4], Chan, Hu, and Plant's Input Estimation Method [5], and Goff, Black, and Beck's variable dimension approach [6] directly append accelerations to the state vector for estimation when a maneuver is detected through residuals, but such methods require observation throughout a continuous maneuver. Patera's space event detection method [7] focuses more on quick events in an astrodynamics context, so it tends to neglect smaller maneuvers and natural dynamics mismodeling as well as being limited in application. Hill's detection method [8], though effective, is based solely on optical tracklets, which limits its application to certain tracking problems. Lee and Hwang's multiple model estimation based method [9] requires the user to predefine what maneuvers to test for and it requires a tuning parameter, so it is not automated in the manner we desire for this study.

Holzinger, Scheeres, and Alfriend [10] addressed the prob-

lems of object correlation, maneuver detection, and maneuver characterization for data-sparse environments by implementing a Control Distance Metric based on a quadratic optimal control policy. Singh, Horwood, and Poore [11] adapted the Control Distance Metric approach by using a minimum-fuel cost function. Lubey and Scheeres [14] adapted these approaches to estimate mismodeled natural dynamics using optimal control policies. This paper uses this optimal control framework along with the Optimal Control Based Estimator and adapts them into an adaptive filter formulation capable of automatic state estimation, control estimation, maneuver detection, maneuver reconstruction, and natural dynamics estimation.

In this paper we develop the adaptive OCBE, and demonstrate its use through numerical simulations. In Section II we summarize the Optimal Control Based Estimator - specifically, the linear version of the estimator. In Section III we summarize the maneuver detection properties of this estimator, as they lie at the heart of the adaptive algorithm. In Section IV we develop the central algorithm of this paper - the Adaptive Optimal Control Based Estimator. In Section V we demonstrate the algorithm with realistic tracking scenarios that include unmodeled maneuvers. Finally, we summarize the paper and provide concluding remarks in Section VI.

II. The Optimal Control Based Estimator

The focus of this paper is the adaptive OCBE, but in order set up this algorithm we will provide a brief summary of the Ballistic Linear OCBE (BL-OCBE) in this section. More in depth discussions are provided in Refs. [2] and [3].

The OCBE is derived from a Bolza type cost function with an initial boundary cost (K_{k-1} - the a priori term), a final boundary cost (K_k - the measurement term), and Lagrangian that is integrated over the time of flight ($\mathcal{L}$ - the dynamics term) as shown in Eq. 1.

$$\begin{aligned}\mathcal{J}(\mathbf{x}_{k-1},\mathbf{x}_k,\mathbf{u}(t)) =& K_{k-1}(\mathbf{x}_{k-1},t_{k-1}) + K_k(\mathbf{x}_k,t_k) \\ &+ \int_{t_{k-1}}^{t_k} \mathcal{L}(\mathbf{x}(\tau),\mathbf{u}(\tau),\tau)\,d\tau\end{aligned} \tag{1}$$

In this notation $\mathbf{x}$ refers to the state of the system, $\mathbf{u}$ refers to control inputs into the system, and the subscripts indicate at what epoch the values are evaluated ($k-1$ = initial epoch [t_{k-1}] and k = final epoch [t_k]). To fully define the system, we make the following definitions: $\mathbf{x} \in \mathbb{R}^n$; $\mathbf{u} \in \mathbb{R}^m$; and K_0, K_f, and $\mathcal{L}$ are scalar functions. The goal is to determine a state and control trajectory that minimizes this cost function.

The costs in this cost function are shown below.

$$\begin{aligned}K_{k-1}(\mathbf{x}_{k-1},t_{k-1}) =& \\ &\frac{1}{2}\left(\bar{\mathbf{x}}_{k-1|k-1}-\mathbf{x}_{k-1}\right)^T \bar{P}^{-1}_{k-1|k-1}\left(\bar{\mathbf{x}}_{k-1|k-1}-\mathbf{x}_{k-1}\right)\end{aligned} \tag{2}$$

$$K_k(\mathbf{x}_k,t_k) = \frac{1}{2}\left(\mathbf{Y}_k - h(t_k,\mathbf{x}_k)\right)^T R_k^{-1}\left(\mathbf{Y}_k - h(t_k,\mathbf{x}_k)\right) \tag{3}$$

$$\begin{aligned}\mathcal{L}(\mathbf{x}(t),\mathbf{u}(t),t) &= \frac{1}{2}\mathbf{u}(t)^T\tilde{Q}(t)^{-1}\mathbf{u}(t) \\ \tilde{Q}(t) &= (t_k - t_{k-1})Q(t)\end{aligned} \tag{4}$$

They are chosen to reflect the information content of problem, such that the estimated state trajectory fully accounts for a priori state knowledge (Eq. 2), measurements (Eq. 3), and confidence in the dynamic model (Eq. 4).

In terms of notation we define the inputs into this process as such: $\bar{\mathbf{x}}_{k-1|k-1}$ is the best estimate of the state at t_{k-1} based on observations through t_{k-1} (this convention for the subscript will be used throughout this paper), $\mathbf{Y}_k$ is a vector containing system measurements at t_k, and $h(t,\mathbf{x}(t))$ is the observation-state relationship that maps a given time and state into an equivalent measurement of the system. The a priori state estimate and measurement are defined as Gaussian random variables where the weighting matrices in these cost functions are the covariance matrices of the associated distribution ($\bar{P}_{k-1|k-1}$ and R_k, respectively). The expected values for both random variables are truth (indicated with an asterisk). Furthermore, we define the weighting matrix $Q(t)$ as the covariance of a stochastic-zero mean control input ($\mathbf{w}(t)$) that is uncorrelated in time.

$$E\left[\mathbf{w}(t)\mathbf{w}(\tau)^T\right] = Q(t)\delta(t-\tau) \tag{5}$$

Given that the user does not have knowledge of the presence or form of dynamic mismodeling a priori, the assumed dynamic uncertainty ($\tilde{Q}(t)$) is a parameter that must be adjusted to obtain the best tracking. This is achieved when the assumed dynamic uncertainty is set to be on the same level as the dynamical modeling (if it is present). The Adaptive OCBE focuses on automatically selecting this parameter.

Dynamic constraints ($\dot{\mathbf{x}}(t) = f(t,\mathbf{x},\mathbf{u})$) are enforced in the integral portion of the cost function via a Lagrange multiplier ($\mathbf{p}(t)$) known as the system adjoint. This constraint effectively enforces a nominal model about which control estimates are used to reconstruct dynamic mismodeling. The solution that minimizes this cost function are the initial state, final state, and a control trajectory that minimize deviation from the given pieces of information (as previously defined) such that the initial and final states are connected on a trajectory defined by the enforced dynamics and the estimated control trajectory. This solution is obtained by enforcing the necessary conditions that accompany functional optimization including the Pontryagin Minimum Principle, Transversality conditions, and the state and adjoint dynamical equations that come from reformulating the problem as a Hamiltonian dynamical system. There is no explicit solution to this nonlinear problem so we linearize the problem to obtain a solution. We specify this nominal trajectory to be ballistic (control is zero for all time), and denote values on it with tildes, which results in the BL-OCBE.

Before summarizing the BL-OCBE, it is important to first define linearized notation. Motion in the vicinity of the nominal trajectory is described by the system's State Transition Matrix (STM - Eq. 6), which includes state and adjoint trajectories.

$$\Phi(t_k,t_{k-1}) = \begin{bmatrix} \Phi_{xx}(t_k,t_{k-1}) & \Phi_{xp}(t_k,t_{k-1}) \\ \Phi_{px}(t_k,t_{k-1}) & \Phi_{pp}(t_k,t_{k-1}) \end{bmatrix} \tag{6}$$

As a notational note, when we refer to a portion of the STM without time arguments the assumption is that it is evaluated between t_{k-1} and t_k. In order to make the formulation similar to a standard Kalman Filter, we propagate the a priori state estimate as shown in Eq. 7.

$$\delta\bar{\mathbf{x}}_{k|k-1} = \Phi_{xx}\delta\bar{\mathbf{x}}_{k-1|k-1} \tag{7}$$

This is just a notational convenience to make comparisons to a standard Kalman filter - we still are able to separate dynamic and a priori uncertainty via their separation in the original cost function. The accompanying covariance matrix, which describes the uncertainty in this propagated random variable is given in Eq. 8.

$$\bar{P}_{k|k-1} = \Phi_{xx}\bar{P}_{k-1|k-1}\Phi_{xx}^T - \left(\Phi_{xp}\Phi_{xx}^T\right) \tag{8}$$

This matrix can be shown to be identical to the uncertainty in the propagated state estimate for a Kalman Filter with the effects of process noise included [3]. Measurement information is linearized with respect to the nominal trajectory as described in Eqs. 9 and 10.

$$\delta\mathbf{y}_k = \mathbf{Y}_k - h(t_k, \tilde{\mathbf{x}}(t_k)) \tag{9}$$

$$\tilde{H}_k = \left.\frac{\partial h}{\partial \mathbf{x}}\right|_{(t_k, \tilde{\mathbf{x}}(t_k))} \tag{10}$$

Having defined all necessary notation, the BL-OCBE is defined as shown in Eqs. 11 - 15

$$\delta\hat{\mathbf{x}}_{k-1|k} = \delta\bar{\mathbf{x}}_{k-1|k-1} + L_{k-1}\left(\delta\mathbf{y}_k - \tilde{H}_k\delta\bar{\mathbf{x}}_{k|k-1}\right) \tag{11}$$

$$\delta\hat{\mathbf{x}}_{k|k} = \delta\bar{\mathbf{x}}_{k|k-1} + L_k\left(\delta\mathbf{y}_k - \tilde{H}_k\delta\bar{\mathbf{x}}_{k|k-1}\right) \tag{12}$$

$$\delta\hat{\mathbf{p}}_{k-1|k} = -\bar{P}_{k-1|k-1}^{-1}L_{k-1}\left(\delta\mathbf{y}_k - \tilde{H}_k\delta\bar{\mathbf{x}}_{k|k-1}\right) \tag{13}$$

$$L_k = \bar{P}_{k|k-1}\tilde{H}_k^T\left(R_k + \tilde{H}_k\bar{P}_{k|k-1}\tilde{H}_k^T\right)^{-1} \tag{14}$$

$$L_{k-1} = \bar{P}_{k-1|k-1}\Phi_{xx}^T\tilde{H}_k^T\left(R_k + \tilde{H}_k\bar{P}_{k|k-1}\tilde{H}_k^T\right)^{-1} \tag{15}$$

In this notation, hats indicate values that are optimized relative to the given cost function. These include state estimates at both epochs, and an adjoint estimate at the initial estimate (the adjoint is used to calculate the optimal control policy as described in the following section).

We complete the definition of the BL-OCBE by providing estimates of the uncertainty in the state estimates as shown in Eqs. 16 and 17.

$$\hat{P}_{k-1|k} = \bar{P}_{k-1|k-1} - L_{k-1}\left(R_k + \tilde{H}_k\bar{P}_{k|k-1}\tilde{H}_k^T\right)L_{k-1}^T \tag{16}$$

$$\hat{P}_{k|k} = \left(I - L_k\tilde{H}_k\right)\bar{P}_{k|k-1}\left(I - L_k\tilde{H}_k\right)^T + L_kR_kL_k^T \tag{17}$$

Further analysis of the BL-OCBE will show that the measurement epoch state estimate is identical to a Kalman Filter with process noise and the state estimate at the a priori epoch is equivalent to a smoothed Kalman Filter estimate. As such, we can conclude that the linear OCBE is a linear-unbiased-minimum variance estimator at both epochs. The estimated adjoint is used to determine the optimal control policy that links these two states. After calculating it, analysis of this control policy can yield information on the mismodeled dynamics within the system.

III. Maneuver Detection and Reconstruction

The uniqueness of the OCBE lies in the dynamics it estimates simultaneously with the state. These estimates may be analyzed to identify and reconstruct dynamic mismodeling so that the dynamic model is more accurate for future estimation and propagation. Maneuver detection is the general term we use for dynamic mismodeling identification regardless of whether that mismodeling is is from natural dynamics or active control. Maneuver detection, like estimation, is a statistical process that uses knowledge in the dynamics to determine how statistically significant the estimated control policies are.

The control policies are generated via the adjoint estimates per the linearized Pontryagin Minimum Principle as shown in Eq. 18

$$\mathbf{u}(t) = \delta\mathbf{u}(t) = -\tilde{Q}(t)\frac{\partial f}{\partial \mathbf{u}}^T\Phi_{pp}(t, t_{k-1})\delta\hat{p}_{k-1} \tag{18}$$

These control policies are reconstructions of unknown dynamics, but they are influenced by noise from a priori uncertainty, measurement uncertainty, and dynamic uncertainty so it is necessary to determine whether they are just noise or something deterministic. Only after determining a control policy to be statistically significant can we accept the hypothesis that it is representative of dynamic mismodeling within the system.

To determine whether a control policy estimate is statistically significant we utilize the control distance metric of Holzinger, Scheeres, and Alfriend [10]. The control distance metric in this paper is slightly modified from the original to be a weighted metric (Eq. 19) in order to make the metric equivalent to the integrated Lagrangian portion of the OCBE cost function.

$$D_C(\tilde{Q}(t)) = \int_{t_{k-1}}^{t_k}\frac{1}{2}\mathbf{u}(\tau)^T\tilde{Q}(\tau)^{-1}\mathbf{u}(\tau)d\tau \tag{19}$$

Our goal is to determine the mean and variance of the distance metric as a function of the uncertainties within the problem (a priori state, measurement, and dynamics). We then use these statistics to set a a statical threshold such that any metric calculated that exceeds the threshold is deemed statistically significant - meaning we accept the hypothesis that the control policy is representative of some deterministic uncompensated dynamic mismodeling. It is important to distinguish this hypothesis with the qualifier uncompensated because if the assumed dynamic uncertainty is set properly (or too large) no maneuver will be detected. However, if we set the threshold using a predefined dynamical noise floor (i.e. the smallest level of dynamical uncertainty that is detectable) maneuvers may still be detected relative to this alternate threshold as we properly adjust the assumed dynamical uncertainty. More details on this are provided in the following section.

To properly determine the mean and variance of the control distance metric in terms of the uncertainties in our information content we sub the control policy estimate into the distance metric equation, and then take the appropriate expectations. Subbing the expression for the estimated adjoint (Eq. 13) into the control estimate (Eq. 18), and then subbing this result into the distance metric (Eq. 19) we obtain the expressions shown in Eqs. 20 and 21.

$$D_C(\tilde{Q}(t)) = \left(\delta\mathbf{y}_k - \tilde{H}_k\delta\bar{\mathbf{x}}_{k|k-1}\right)^T M_k \left(\delta\mathbf{y}_k - \tilde{H}_k\delta\bar{\mathbf{x}}_{k|k-1}\right) \quad (20)$$

$$M_k(\tilde{Q}(t)) = -\frac{1}{2}L_k^T\bar{P}_{k|k-1}^{-1}\Phi_{xp}\Phi_{xx}^T\bar{P}_{k|k-1}^{-1}L_k \quad (21)$$

These include simplifications that arise from the equivalency of process noise and the BL-OCBE propagated state uncertainty (Eq. 8). It is worth nothing that the effects of the assumed dynamic uncertainty propagate through the Φ_{xp} matrix, which also influences $\bar{P}_{k|k-1}$ and L_k (see Eqs. 8 and 14, respectively).

The innovations are zero mean with a known covariance according the definitions we have made. Knowing this, we obtain the following mean and variance statistics on the distance metric (Eqs. 22 and 23) via stochastic equations for quadratic forms [10].

$$\mu_{D_C}(\tilde{Q}(t)) = Trace\left[M_k\left(R_k + \tilde{H}_k\bar{P}_{k|k-1}\tilde{H}_k^T\right)\right] \quad (22)$$

$$\sigma_{D_C}^2(\tilde{Q}(t)) = 2\left(Trace\left[\left(M_k\left(R_k + \tilde{H}_k\bar{P}_{k|k-1}\tilde{H}_k^T\right)\right)^2\right]\right) \quad (23)$$

Making the assumption that the distance metric may be modeled as a Gaussian random variable with this mean and variance, we can set a threshold ($\Theta_C(\tilde{Q}(t))$) at a particular z-score (e.g. $z = 1.96$ for a 95% confidence level). If we make the hypothesis that no unmodeled accelerations are present in the system, then exceeding this threshold invalidates this hypothesis, signaling a detected maneuver (uncompensated mismodeled dynamics). Because these metrics are positive definite there will be errors that arise from the Gaussian assumption, but we have found these errors to be negligible in practice. The method could be modified to use another profile to model the uncertainty in the distance metric, but the algorithm would have to be numerical as opposed to the analytical result that comes from a Gaussian assumption.

As indicated by the functional dependance, the level of assumed dynamic uncertainty ($\tilde{Q}(t)$) largely controls whether a maneuver is detected. This is because, as mentioned, maneuvers are termed uncompensated mismodeled dynamics. When the assumed dynamic uncertainty is appropriately tuned, then the system properly compensates for the mismodeled dynamics given that this process injects the proper amount dynamic uncertainty into the system. The reconstruction of the maneuver (Eq. 18) then may be used to analyze the mismodeled dynamics.

Beyond just detecting a one-time event, it is also possible to detect continuous mismodeling (e.g. atmospheric drag or solar radiation pressure mismodeling). Generally, this manifests as a series of many detected maneuvers in a row, or just frequent detections (if the force is small enough not to build up error over smaller observation gaps). One-time actuated maneuvers tend to be one-time events in maneuver detection space (though it may take a few observations before calming down if they are closely spaced), and these event tend to be larger since orbital maneuvers tend to be larger than mismodeled perturbations. This designation is important to make when approaching reconstruction of the unknown dynamics. Lubey and Scheeres [14] demonstrated a method that may be used to estimate natural dynamics out of optimal control estimate maneuver reconstructions.

The OCBE is set up such that accounting for dynamics uncertainty and providing reconstructions of mismodeled dynamics are natural properties of it. Maneuver detection is a simple extension of these properties, and as can be seen all of the quantities needed to perform maneuver detection are already pieces of the estimations process (i.e. no other integrations or complex computational processes are required). In the next section, we develop a method to leverage these properties of the OCBE toward creating a method that automates the algorithm such that it will no longer require the user to select an assumed dynamical uncertainty at each measurement epoch.

IV. The Adaptive Optimal Control Based Estimator

The OCBE is an accurate state and dynamics estimator, but this accuracy relies on appropriate selection of the assumed dynamic uncertainty. It should reflect the true mismodeling in the system. If too large of a value is used, then too much uncertainty is injected into the system resulting in degraded performance, and artificially high uncertainty in state and dynamics estimates. If too low of a value is used, then uncompensated mismodeled dynamics are still present in the system. These have deterministic trends that can often lead to filter divergence. Given that the user generally has no a priori knowledge of maneuvers, and that mismodeled dynamics can drastically change over time and between observations it is infeasible for a human to be in the loop for complex systems with many targets and observations such as is the case with SSA. Using the maneuver detection properties of the OCBE we are able to design a unique automation method in order to turn the OCBE into and adaptive estimator, which is capable of addressing the complexity concerns of SSA surveys.

While there is often no priori knowledge of maneuvers, it was shown that the OCBE can detect their presence as well as determine when they are fully compensated for. This automation procedure is based upon this maneuver detection property. The algorithm self adjusts the assumed dynamic uncertainty to ensure that all mismodeled dynamics are properly compensated for by finding the point where the distance metric equals the mean of the distribution (as this is the best estimate of the anticipated divergence). This process requires no user input beyond initial parameters, which are established before any measurements are processed.

To simplify the development of this automation procedure we limit the assumed dynamic uncertainty to have a single degree of freedom (σ_Q) as shown in Eq. 24.

$$\tilde{Q}(t) = \sigma_Q^2 (t_k - t_{k-1}) I \tag{24}$$

As it is assumed that the user has no knowledge of any maneuvers before processing measurements, this assumption is justified because it applies equal amount of error in each direction, and it assigns no time dependence to the noise. The method may be modified to add more degrees of freedom (e.g. more components of the assumed dynamic uncertainty matrix), but for this discussion we will limit it to the 1-dimensional case. In terms of notation, we will refer to this scalar parameter (σ_Q) as the assumed dynamic uncertainty as well.

This general idea behind this method relies on the assumption there exists a point where the distance metric and mean of the spread are equal. This is not a reliable assumption for an operational algorithm, thus it is necessary to either prove existence for an arbitrary case, or find an example where the solution does not exist in order to prove that existence is not guaranteed. In the latter case it would then be important to develop an alternate solution to default to. Through testing we have found that solutions do tend to exist when there are mismodeled dynamics in the system that are significant enough to detect or when measurement and a prior state errors are outliers. An example of this is shown in Fig. 1 where a unmodeled maneuver is present in the observation gap. There is a clear intersection between the metric and the mean curves as functions of the assumed dynamic uncertainty, thus indicating a solution exists.

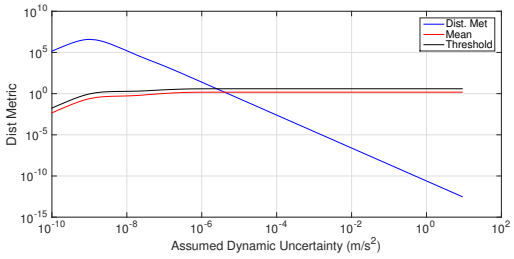

Fig. 1. Distance metric, mean, and threshold as function of the assumed dynamic uncertainty for a case where the adaptive solution exists (at the intersection of the distance metric and mean functions).

There are occasions when a solution does not exist, such as the example shown in Fig. 2. These tend to occur when the dynamics are either modeled perfectly or the mismodelings are not significant enough to cause large deviations across the observation gap and the measurement and a priori state errors are not outliers.

Because there are occasions where a solution exists, we must define a default solution for such occasions. A dynamic noise floor ($\sigma_{Q,NF}$) solves this problem. The dynamic noise floor is a parameter set by the user (before any measurements are processed) that sets a floor on how small of mismodelings the algorithm can detect. Any mismodelings below this floor

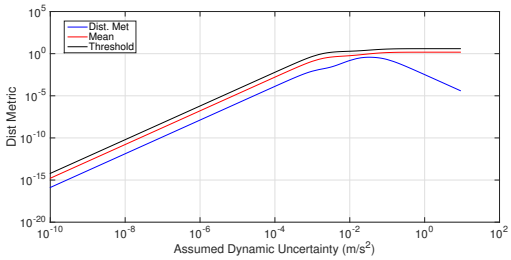

Fig. 2. Distance metric, mean, and threshold as functions of the assumed dynamic uncertainty for a case where the adaptive solution does not exist (no intersection between distance metric and mean functions).

are assumed to be just noise within the system. When a solution does not exist we default to this noise floor to account for any mismodelings that are present that are less than the floor while injecting a minimal amount of additional uncertainty into the system. As a general rule of thumb, if the distance metric is less than the mean at the noise floor, then the solution does not exist.

If the metric is greater than the mean at the noise floor, then a solution will exist. To obtain that solution we use a numerical Newton-Secant Root finder. This provides a more simple implementation with respect to other root finders since it does not require derivatives of functions of interest. Additionally, the problem tends to be quite linear in log-log space near a solution, so the Newton-Secant method converges quite quickly. The first step is to establish bounds of the solution. Starting at the noise floor bounds are placed an order of magnitude from one another and moved up with each iteration until the mean-metric difference is negative at one bound and positive at another. Calculating the distance metric and mean at all of these values of the assumed dynamic uncertainty is quite simple when using Eq. 25.

$$\begin{aligned} g(\sigma_Q) &= \Phi_{xp}\Phi_{xx}^T \\ &= -\int_{t_{k-1}}^{t_k} \Phi_{xx}(t_k,\tau)\frac{\partial f}{\partial \mathbf{u}}\tilde{Q}(\tau)\frac{\partial f}{\partial \mathbf{u}}^T \Phi_{xx}^T(t_k,\tau)d\tau \\ &= \left(\frac{\sigma_Q}{\sigma_{Q,NF}}\right)^2 g(\sigma_{Q,NF}) \end{aligned} \tag{25}$$

The only term in the metric and mean equations that is a function of the assumed dynamic uncertainty is the STM product in the propagated a priori uncertainty ($\Phi_{xp}\Phi_{xx}^T$). Other matrices in the maneuver detection process (e.g. L_k and $\bar{P}_{k|k-1}$) are also functions of this matrix, so these must be adjusted with each new assumed dynamic uncertainty.

With the bounds set, we can initiate the root finder. The algorithm is shown in Eqs. 26 and 27.

$$\begin{aligned} v &= \log(\sigma_Q) \\ z(v) &= \log[D_C(v)] - \log[\mu_{D_C}(v)] = \log\left[\frac{D_C(v)}{\mu_{D_C}(v)}\right] \end{aligned} \tag{26}$$

$$v_{i+1} = v_i^{(-)} - z\left(v_i^{(-)}\right)\left(\frac{v_i^{(+)} - v_i^{(-)}}{z\left(v_i^{(+)}\right) - z\left(v_i^{(-)}\right)}\right) \tag{27}$$

$$\text{if } z(v_{i+1}) > 0 : v_{i+1}^{(-)} = v_{i+1} \text{ and } v_{i+1}^{(+)} = v_i^{(+)}$$

$$\text{else } : v_{i+1}^{(+)} = v_{i+1} \text{ and } v_{i+1}^{(-)} = v_i^{(-)}$$

In this notation the (−) and (+) subscripts indicate the lower and upper bounds, respectively. The algorithm should be iterated until the metric and mean difference converges within a predefined tolerance ($|\mu_{D_C}(\sigma_{Q_{i+1}}) - D_C(\sigma_{Q_{i+1}})| / \mu_{D_C}(\sigma_{Q_{i+1}}) < \Delta_{tol}$). Once the process has converged we set the adaptive solution ($\hat{\sigma}_Q$) as shown in Eq. 28.

$$\hat{\sigma}_Q = 10^{v_{i+1}} \tag{28}$$

To protect from the influence of outliers in the measurement and a priori state errors we set another parameter to cap the assumed dynamic uncertainty ($\sigma_{Q,max}$). This helps to prevent divergence due to chasing noise in the system. If a metric is greater than the mean at the noise floor yet less than the threshold we apply this cap - this ensures that maneuvers are always addressed (though a cap may also be placed on maneuvers if desired). If the solution exceeds this cap we generally default to the noise floor, though one may also defer to the cap (especially if the cap is placed on maneuver events as well).

Figure 3 provides a visualization of this automation algorithm as incorporated into the OCBE, thus creating the Adaptive OCBE. All contingencies are accounted for such that the algorithm will always output a solution. Before the algorithm is started it simply requires the user to define the noise floor and maximum assumed dynamic uncertainty. After this the algorithm runs fully automated.

V. Numerical Simulations

In this section, we provide a demonstration of the abilities of the Adaptive OCBE by applying it to system with mismodeled dynamics. Specifically, we apply it to a system in which a spacecraft in Geosynchronous Earth Orbit (GEO) is tracked via ground stations as it executes stationkeeping maneuvers (unknown to the estimator) to correct for latitude and longitude deviations from the nominal orbit due to non-Keplerian perturbations (e.g. non-spherical Earth gravity, solar radiation pressure, third-body gravity, etc.).

The stationkeeping maneuvers come in two varieties: (1) East-West (EW) maneuvers that correct longitude errors and (2) North-South (NS) maneuvers that correct latitude errors. These operate independently since longitude drift tends accumulate much faster than latitude drift. Maneuvers are developed from a timed-fixed (12 hour) optimal control law that minimizes a quadratic control cost (as is used for the distance metric). While this creates a strong similarity between the controls and what we use to estimate them, we have found in separate analysis that using different maneuver models yields similar results (such as using impulsive models).

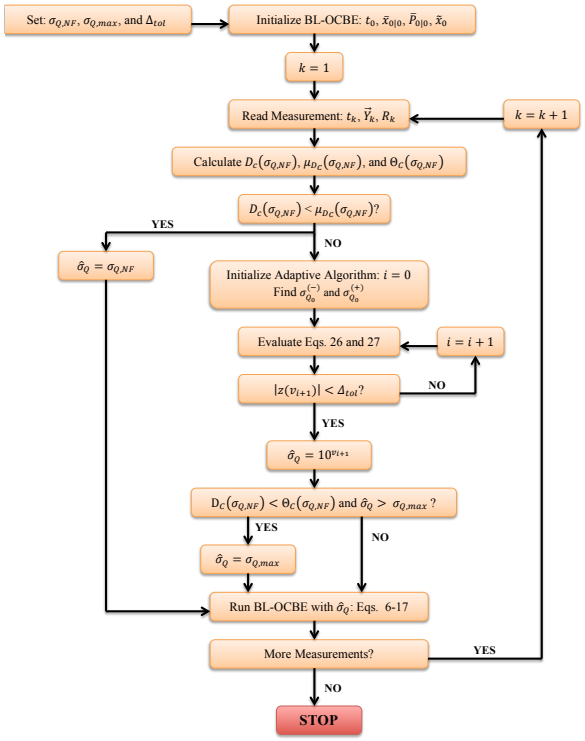

Fig. 3. Flowchart defining the Adaptive Optimal Control Based Estimator algorithm.

The nominal GEO orbit at 60 degrees longitude is visible to fixed ground station at all times, but we design the measurements such that they are only captured once a night for a two hour period (one measurement every 100 seconds in this period) to reflect reality. This also provides a mixture of data rich and data sparse periods to identify how this algorithm works in each phase. Range and optical (azimuth and elevation angles) data are taken at each epoch. Range observations include 1 m Gaussian error, and angles observations include 1 arcsecond Gaussian error for each simulation. The adaptive parameters are set to 10^{-12} m/s^2 for the dynamic noise floor ($\sigma_{Q,NF}$), 10^{-6} m/s^2 for the maximum assumed dynamic uncertainty ($\sigma_{Q,max}$), and 10^{-10} for the convergence tolerance (Δ_{tol}).

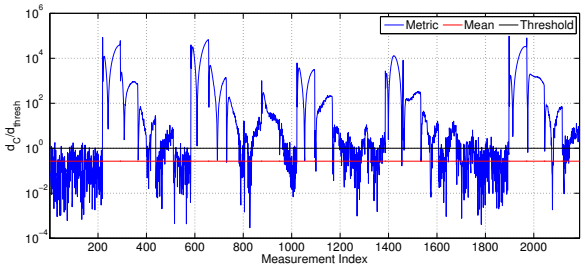

Fig. 4. Ratio of control distance metrics and metric threshold at each measurement epoch using a constant assumed dynamic uncertainty ($\sigma_Q = 10^{-8}$ m/s^2).

Observations are taken over the course of 1-month, during which 6 maneuvers occur (5 EW and 1 NS). Using a constant level of assumed dynamic uncertainty (10^{-8} m/s^2), we can see how the metrics diverge in the presence of maneuvers (Fig. 4). The six events are clear in the results (indicated by exceeding the threshold), but it not clear when they begin and where the next begins. Proper adjustment of the assumed dynamic uncertainty can remove this ambiguity. This is accomplished by application of the Adaptive OCBE.

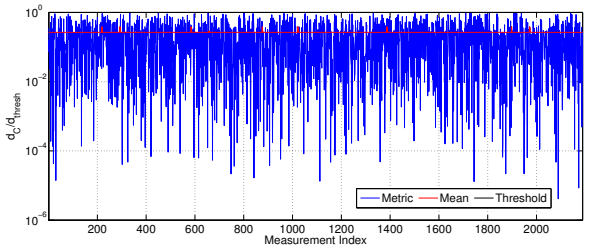

Fig. 5. Ratio of control distance metrics and metric threshold at each measurement epoch using the Adaptive OCBE.

Application of the Adaptive OCBE yields the metric ratios as shown in Fig. 5. This plot includes the ratios relative to a threshold at the tuned assumed dynamic uncertainty, thus no metric ratio should exceed 1. This is exactly what we see. The spread about the mean is appropriate and their are no outliers, thus indicating we are keeping track of the spacecraft. The tuned assumed dynamic uncertainty is shown in Fig. 6. While there are many spikes in this response only a few stand out - these represent the real maneuvers whereas the other spikes correspond to accumulating error due to linearization as well as outliers in the measurements. Groupings of spikes correspond to detecting an active maneuver that is observed during an observation window. Of the six maneuvers, four are observed during observation windows. The assumed dynamic uncertainties do not respond during all of these measurement epochs, because a low thrust maneuver does not accumulate enough error in a 100 second observation gap to be detected given the uncertainties in the observations.

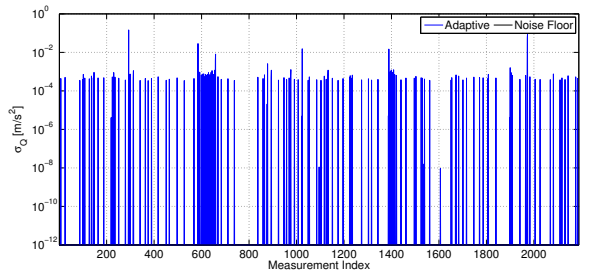

Fig. 6. Assumed dynamic uncertainty used at each measurement epoch using the Adaptive OCBE.

The algorithm cannot discern small maneuvers over short observation gaps, but it clearly discerns maneuvers as a whole. They are most obvious when comparing the metrics against a threshold calculated at the noise floor (Fig. 7). The spikes in the plot either correspond to the beginning or end of a maneuver (with small spikes for detections in between) or an entire maneuver (if it executes entirely in an observation gap). All six events stand out clearly.

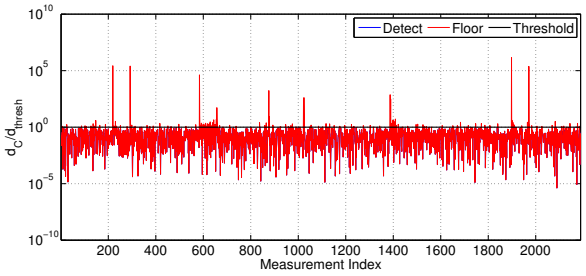

Fig. 7. Ratio of control distance metrics calculated at the adaptive assumed dynamic uncertainty and the metric threshold calculated at noise floor for each measurement epoch.

The true and estimated unweighted distance metrics are plotted in Fig. 8. These results confirm the detections made in the previous plots. We also find that the estimated metrics are of similar order of magnitude to truth. Unfortunately, there are also many false detection of a slightly lesser order of magnitude. These are due to the linear nature of the filter in this nonlinear system, which results in accumulating a error that is corrected with false detections. Also, the outliers in measurements and Gaussian assumption on the distance metric contribute. For future studies, a nonlinear version of the estimator will be approached as well as a non-Gaussian metric in order to make these detections even more accurate.

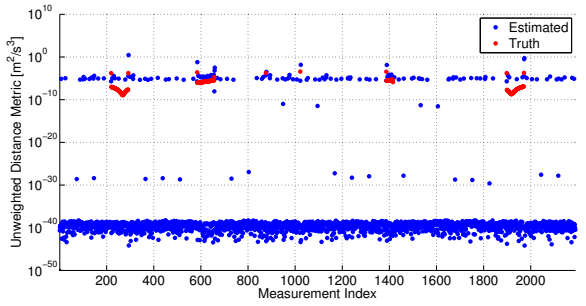

Fig. 8. Unweighted estimated and true control distance metrics for each measurement epoch.

Further information may be gleaned from the maneuver reconstructions (Fig. 9). The type of maneuver is evident based on whether it is dominated by in plane accelerations (radial and along-track) or out-of-plane accelerations (cross-track). Of the six maneuvers it is clear that five are EW and the other is NS, which agrees with truth.

Finally, the most important aspect of an effective estimator is that it keeps track of the object. The position and velocity deviations with a 3-sigma envelope are given in Fig. 10. We find that the deviations are well-bounded, except in a couple

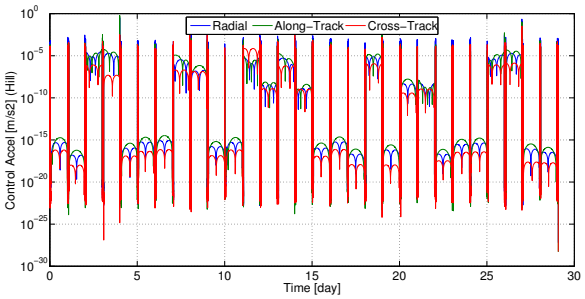

Fig. 9. Control estimates as function of time throughout the entire observation arc.

of cases but tracking is regained immediately afterward. This indicates algorithm successfully works even in the presence of unknown maneuvers.

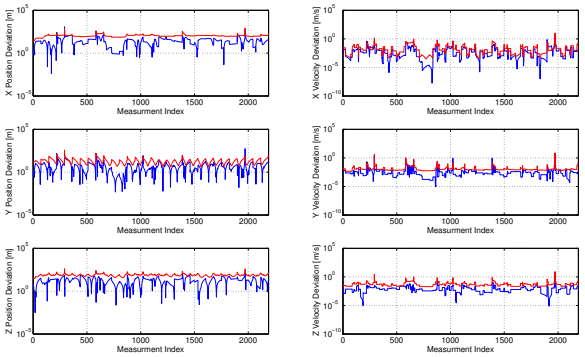

Fig. 10. Smoothed state deviations (relative to truth) with uncertainty in ECI frame. (Red) The 3-sigma uncertainty and (Blue) smoothed state estimate deviation with respect to truth.

This example has shown this algorithm's ability to successfully identify maneuvers, compensate for them, and characterize them. There are slight issues with identifying low thrust events at a high data rate, but the algorithm easily identifies maneuvers as a whole.

VI. Conclusions and Future Work

In this paper we developed the Adaptive Optimal Control Based Estimator (OCBE) - an algorithm that automatically tracks a system with mismodeled dynamics while simultaneously providing information about the dynamic mismodeling. This information includes detection of mismodeling events and reconstructions of those events. The automation of this algorithm makes it feasible to use with highly complex systems such as astrodynamics-based ones - the focus of this paper.

The automation of the Adaptive OCBE is based on maneuver detection properties of the algorithm. Essentially, the assumed dynamic uncertainty parameter (a parameter set by the user when not automated) is chosen to completely compensate for any mismodeled dynamics, thus ensuring the filter does not diverge in the presence of a maneuver. This effectiveness of this method was demonstrated via a numerical simulation in which the Adaptive OCBE was able to successfully keep track of and provide dynamics information on a spacecraft undergoing stationkeeping maneuvers, which were unknown to the estimator dynamics. The adaptive OCBE detected each of these events, and was even able to characterize their purpose.

In terms of future work, we would like to improve this algorithm by removing the limitations that accompany linear and Gaussian assumptions. Specifically we will pursue a nonlinear version of the estimator. While the Adaptive OCBE resists divergence due to mismodeled dynamics, it would be more accurate if it were not linearized. Additionally, we would like to remove the Gaussian assumption on the distance metrics. This would ensure more accurate detection, though it will require a numerical method as opposed to the analytical method developed in this paper.

Acknowledgment

This work was supported by a NASA Office of the Chief Technologist's Space Technology Research Fellowship.

References

[1] Shoots, D. & Anz-Meador, P., *Orbital Debris Quarterly News*, National Aeronautics and Space Administration, Vol. 19, No. 1, January 2015.

[2] Lubey, D.P. & Scheeres, D.J., *Combined Optimal Control and State Estimation for the Purposes of Maneuver Detection and Reconstruction*, Proceedings of the 2014 American Control Conference, Portland, OR, 2014.

[3] Lubey, D.P. & Scheeres, D.J., *Supplementing State and Dynamics Estimation with Information from Optimal Control Policies*, Proceedings of the 17th International Conference on Information Fusion, July 2014.

[4] Bar-Shalom, Y. & Birmiwal, K., *Variable Dimension Filter for Maneuvering Target Tracking*, Aerospace and Electronic Systems, Vol. 18, No. 5, pp. 621-629, 1982.

[5] Chan, Y.T., Hu, A.G.C., & Plant, J.B., *A Kalman Filter Based Tracking Scheme with Input Estimation*, Aerospace and Electronic Systems, Vol. 15, No. 2, pp. 237-244, 1979.

[6] Goff, G.M., Black, J.T., & Beck, J.A., *Orbit Estimation of a Continuously Thrusting Spacecraft Using Variable Dimension Filters*, AIAA Guidance, Navigation, and Control Conference, January 2015.

[7] Patera, R.P., *Space Event Detection Method*, Journal of Spacecraft and Rockets, Vol. 45, No. 3, 2008.

[8] Hill,K., *Maneuver Detection and Estimation with Optical Tracklets*, Proceedings of the 2014 Advanced Maui Optical and Space Surveillance Technologies Conference, September 2014.

[9] Lee, S. & Hwang, I., *Interacting Multiple Model Estimation for Spacecraft Maneuver Detection and Characterization*, AIAA Guidance, Navigation, and Control Conference, January 2015.

[10] Holzinger, M.J., Scheeres, D.J., & Alfriend, K.T., *Object correlation, maneuver detection, and characterization using control distance metrics*, Journal of Guidance, Control, and Dynamics, Vol. 35, No. 4 (2012), pp. 1312-1325. doi: 10.2514/1.53245

[11] Singh N., Horwood J.T., & Poore A.B., *Space Object Maneuver Detection Via a Joint Optimal Control and Multiple Hypothesis Tracking Approach*, Proceedings of the 22nd AAS/AIAA Space Flight Mechanics Meeting, January 2012.

[12] Athans, M. & Tse, E., *A Direct Derivation of the Optimal Linear Filter Using the Maximum Principle*, IEEE Transactions on Automatic Control, Vol. 12, No. 6, December 1967, pp. 690-698. doi: 10.1109/TAC.1967.1098732

[13] Rao, C.V., Rawlings, J.B., & Mayne, D.Q., *Constrained State Estimation for Nonlinear Discrete-Time Systems: Stability and Moving Horizon Approximations*, IEEE Transactions on Automatic Control, Vol. 48, No. 2, February 2003, pp. 246-258. doi: 10.1109/TAC.2002.808470

[14] Lubey, D.P. & Scheeres, D.J., *Identifying and Estimating Mismodeled Dynamics via Optimal Control Problem Distance Metrics*, Journal of Guidance, Control, and Dynamics, Vol. 37, No. 5, (2014), pp. 1512-1523. doi: 10.2514/1.G000369